COBEM 99
XV Congresso Brasileiro de Engenharia Mecânica
15th Brazilian Congress of Mechanical Engineering
22 - 26 de Novembro de 1999 / November 22 - 26, 1999 Águas de Lindóia, São Paulo,

PATTRERNS OF FLOW –LIKE IMAGES REVELED BY A DIGITAL IMAGE PROCESSING

Paulo Sérgio Silva Rodrigues
Arnaldo de Alburquerque Araújo
Universidade Federal de Minas Gerais, Departamento de Ciência da Computação
Av. Antônio Carlos,6627 - Pampulha - Cep.31270-901, Belo Horizonte, MG, Brasil
e-mail: pssr@dcc.ufmg.br
Marcos Pinotti Barbos
Universidade Federal de Minas Gerais, Departamento de Engenharia Hidráulica e Recurso Hídricos
Av. Antônio Carlos,6627 - Pampulha - Cep.31270-901, Belo Horizonte, MG, Brasil
e-mail: pinotti@cce.ufmg.br

Abstract. *Automatic Systems to fluid flow visualization can help in solution of several Fluid Dynamic Phenomena. Usually, these systems can be concerned of three fundamental steps: data acquisition, processing and result display. There are several ways to achieve the first step, which can be grouped as follows: simulation of mathematics elements, and detection/description of fluid flow patterns characteristics. The detection/description is done in real images captured in laboratory experiments and can form the basis of moderns fluid flow visualization systems. These fluid flow patterns can be of several classes which, in Dynamical Systems Theory, are called Critical Points or Singular Points. Even in this theory, these patterns are modeled as different equation systems too. These models can revel intrinsic aspects of fluid flow phenomena and are difficult to achieved in real time computation. So, in this paper, we present a new efficient methodology concerning of four steps, which is also part of a larger effort toward fluid flow patterns description. The time required to execute the proposed method is less than the time required for the other methods here discussed. Some examples, where the proposed methodology can be applied, are presented and the results are discussed. Moreover, it is show that the proposed method can find some kind of occluded patterns too.*

Key-Words*: Pattern Analysis, Fluid Flow Images, Pattern Recognition.*

1. INTRODUÇÃO

Flow, even being of water, oil, gas or blood, has patterns which occur repeatedly. The analysis of these patterns may be the basis of several studies in a Fluid Dynamics phenomenon. The fluid flow analysis may be fundamental in a complete system of flow visualization. The traditional form to study flow which occurs in a fluid dynamics phenomenon is through the human observation of photographs and videos taken off from an

in vitro experiment of the flow (Kopiev *et al*, 1996; Martins and J. H. Whitelaw, 1996). But to study the flow comportment through the analysis of their patterns over digital images is still a challenger. Then, recently, a series of methodologies have been proposed to detect several kinds of patterns in fluid flow images (Ford, 1997; Mao, 1992; Rao and Jain, 1992).

Oriented texture patterns can be studied with these proposed methodologies too. Recently, the analysis of oriented textures has been used over images which are not from fluid flow phenomena but flow-like images as remarked by the work published in 1992 by Rao (Rao and Jain, 1992). Rao showed several applications where these oriented textures need to be detected, analysed and described. Some of the mentioned applications are: the analysis of fractograph specimens, petrography(MackKenzie, 1982), defects in wood (Conners *et al*, 1983; . Erteld *et al*, 1964; Panshin *et al*, 1964.), fingerprint identification (Qinghan and Zhaoqi, 1986) and classification of defects arising in semiconductor wafer inspection (Rao and Jain, 1990).

In 1997, Ford (Ford, 1997) proposed a methodology, based in the Dynamical Systems theory to detect flow-like patterns in fluid flow images. Ford achieved good results for a highly oriented flow field and some degree of success for a turbulent flow and occluded patterns. In his work, Ford tried to resolve several problems of previous methodology. Ford's methodology, as in Rao (Rao and Jain, 1992), has two principal parts: computing of oriented texture fields and detection of patterns. Several other methodologies have been proposed for specific patterns as vortices too (Mao, 1992)**.**

Then, the need of development for automated inspection of flow-like patterns has been evident. In the present work we propose a methodology, which is an ongoing work and based in these recent works, to detect patterns in fluid flow images. Our approach has four principal steps and we intend, in the future, to run this method in a complete flow visualization system to study turbulent blood flow outside of cardiac prothesis.

2. PREVIOUS WORKS AND THE PROPOSED METHODOLOGY

As related in the last section, several methodologies have been proposed to detect flow-like patterns in digital images to analyze fluid dynamics phenomena as textured oriented surfaces. We remark two of them. Rao and Jain's methodology (Rao and Jain, 1992) which uses some kind of segmentation, patterns matching and dynamical system estimation to describe critical points in gray level images. The disadvantage of this method is the $O(n^3)$ complexity due to the estimation of dynamical systems parameters over the whole image. Ford proposed a method (Ford, 1997) to detect patterns in fluid flow images and achieved good results for highly oriented images and some degree of success for some turbulent images. Ford's methodology could detect some kind of occlude points and even run over some bad resolution images. To reduce the noise influence, problems due to bad resolution and ambiguities, Ford's work defines a concept of energy *E* for gray levels images. According to his work**,** each point at the image has a value of energy which is proportional to the definition of the direction at this point. Then, *E* is used in many other calculations of the method as a weight of influence for each point. The idea is as follows: if a gray level of a specific point is used to achieve some value, then, points with low energy *E*, and consequently low definitions, will have low influence on the calculus, and vice-versa. The high computational time to estimate *E* and the flow orientation is a disadvantage of the Ford's method too.

2.1 The proposed methodology

The proposed method involves four steps: oriented texture detection; potential critical point location; matching patterns classes and patterns describing. We remark that our method follows the literature tendency on flow-like pattern detection but differs from these related works in some points. Our method detects flow-like patterns through the use of templates to match the patterns and we do not need to estimate the dynamical systems $\boldsymbol{A}$ matrix if we do not wish to describe symbolically the patterns. Any way, at the end of the methodology we include a module to estimate these matrices because some applications do need them. Basically, we try to find points which have high probability to be a critical point and run the remainder of the method only over these candidate points. We advocate that this approach reduces the total amount of computation time.

2.1 Detection of oriented patterns

In Rao and Jain's and Ford's methodologies, at the initial part of the methods, it is used a Gaussian filter to smooth the input image to reduce the noise influence during the flow orientation computation. This approach has the disadvantage to eliminate small features from the original image and may influence the next steps. After the Gaussian soothing, both methods employed some kind of steerables bandpass filters (Freeman and Adelson, 1991; Rao and Jain, 1990) which are a linear combination of *x* and *y* basis filters, to estimate the flow directions in the smoothed image.

In the proposed method, as a first step, we use simple Sobel operators to estimate the flow orientation. This was chosen due to its simplicity and low time computation. The flow direction at each point *(x,y)* is computed as $\theta = arc\tan(Sy/Sx)$, where *Sx and Sy* are the answers of the Sobel operator in the *x*- and *y*-directions, respectively. The output of this first step is a two-dimensional matrix where each point *(x,y)* is the flow direction at the *(x,y)* position on the image. Figure 1 shows an example where we applied the first step of the method. Figure 1.a shows a gray level image where a cylindrical bar inside the fluid flow produces two vortices, a saddle point and an occluded saddle point. The two vortices positions are pointed by the arrows labeled *v*; the position of the saddle point is indicated by an arrow labeled *s* and the occluded saddle point is indicated by an arrow labeled *so*.

Figure 1.b presents the flow directions detected by the Sobel operator over the original image. To avoid clutter, the orientation field is calculated for each point in the image, but it is displayed in a sampled form. Figure 1.c shows the flow fields superimposed to the original image. Obviously, the main output of this first step is not what we showed in Figure 1, but a matrix whose values are the directions of the flow. We make the remainder calculus always over this matrix.

2.2 Potential critical points detection

The second step of the method consists of the detection of the potential critical points in the image. This step reduces considerably the time computation of the remainder method because it selects only points with high probability to be a critical point. So the estimation of the dynamical systems $\boldsymbol{A}$ matrix is done only with the potential critical points and not with all image points.

According to the Dynamical Systems theory (Arrowsmith and Place, 1992; Smale and 1974), around a critical point, the flow directions present monotonic changing, increasing or decreasing. Consider an imaginary circle whose radius presents approximately the size of the pattern we wish to detect. In other words, this circle covers totally the patterns that we are finding, as shown in Fig. 2. According to this theory when we move in a counter-clockwise manner inside this imaginary circle, around a critical point, the flow directions change

monotonicaly as we move from a radius to another. If we have, for example, a node point, this changing is increasing and, in the case of a saddle point, this changing is decreasing.

According to what was above explained, we can establish a special criterion to detect potential candidates to be a critical point. This criterion is as follow. At any *W* circular region of the image, if there is a monotonic changing of the flow directions around the central point of this region, it is considered to be a potential critical point, otherwise, this point is rejected. In this work, we use this criterion to label the potential critical points and make an estimation about the real critical points. This approach is adapted from Ford's paper.

It is obvious that the radius of the circle, or the *W* circular region's size, will have strong influence over the method's results, particularly over the pattern's size. If we choose a small *W* size for the region, we will not detect larger patterns, otherwise, if we choose a large *W* size we probably will have problems to detect small patterns. We try to estimate the pattern's size by estimating the dynamical system *A* matrix for each patterns found.

To detect occluded points, at this step, we establish a threshold for the monotonic changing of the flow directions. In other words, we label as potential critical points all the points which presents this characteristics at 50% inside of the *W* circular regions. Then, we may find critical points 50% occluded. In this paper we call these parameters *Dm* (Degree of monotonicity). For this ongoing work, we are not interested to detect occluded points, although we remark that our method may detect it.

The results achieved in this step may generate a great amount of potential critical points, but even so, this number will be less than the total points originally in the input image. Then, as we just discoursed, this reduces the amount of computation time to the next method's steps.

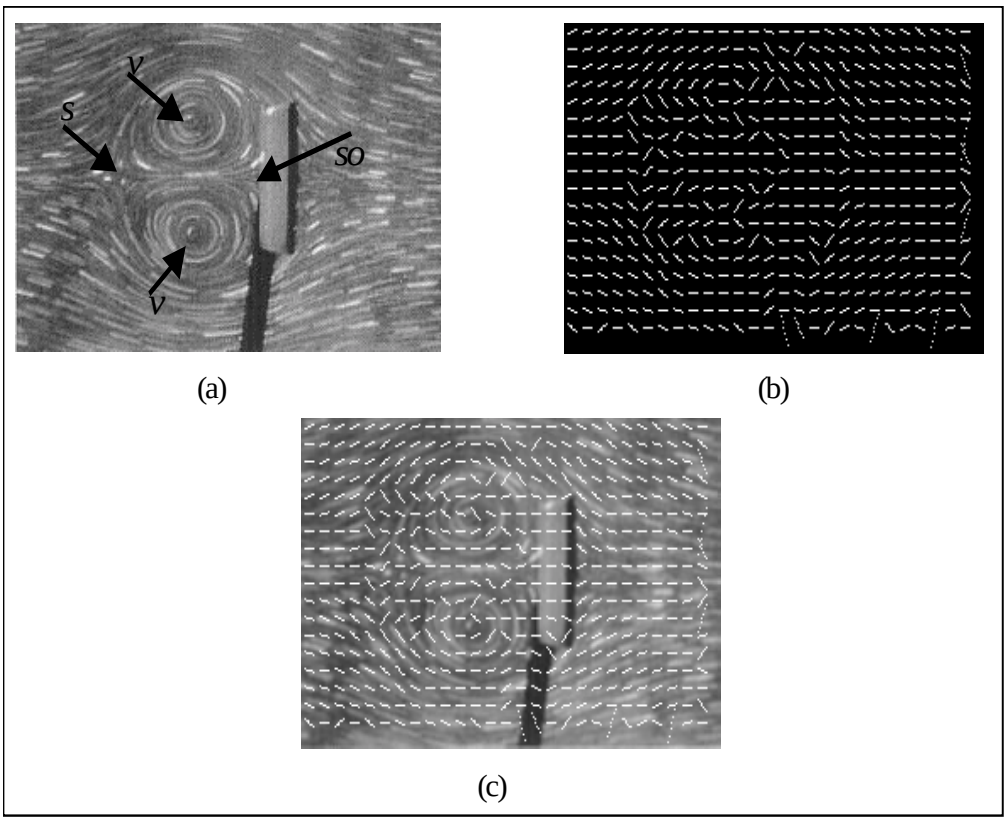

Figure 1. (a) Fluid flow input image with two vortices, indicated by arrows labeled *v*, a saddle point, indicated by an arrow labeled *s* and an occluded saddle point, indicated bay an arrow labeled *so*; (b) flow directions detected by the Sobel operator; and (c) flow fields superimposed to the original image.

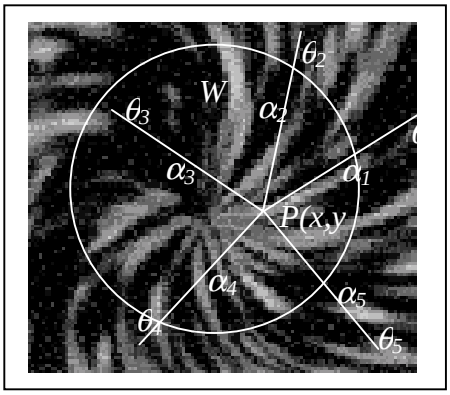

Figure 2. A point *P(x,y)* inside a *W* circular region with five lines, each one with θ_i directions. The flow directions are the α_i values. If we moved, over the circle, from a line which direction is θ_i to another with direction is θ_{i+1} and the flow direction changes monotonicaly (incresing or decrising) then the point *P* is a critical point. In case of this Figure, the flow directions α_i are monotonicaly creasing due the central point *P* of the *W* circular region is at a node point.

2.3 Detecting critical points classes

In this step, which we consider the most important of the method, effectively, we detect the patterns in the image. To do this, we use the labeled points found in the last step. In the detection of the pattern's classes, we use some templates as shown in Fig. 3 for a center point. These templates are, in true, two-dimensional matrices whose positions contain the flow template's direction. Obviously, to avoid clutter, like in Fig. 1, we show the template's directions in a sampled form.

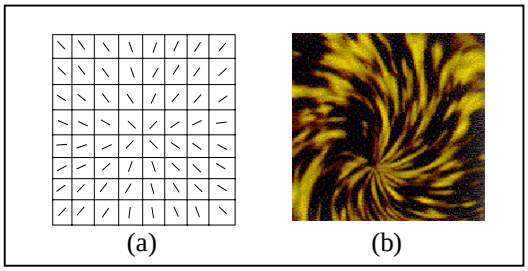

Figure 3. (a) The center template used to match flow-like nodes or spirals images; (b) a flow-like node image.

Each template dimension is fixed as been approximately the size of the expected pattern. In practice, we use as the template's size the same *W* region size in pixels, that we used at the last step to find the potential critical points. We will try to achieve the real dimensions of the patterns in the next step.

These templates, showed in the Fig. 4, are matched only with the potential critical points founded at the last step. We claim that this approach reduces the computational time to detect the patterns. This approach achieves the patterns locations.

In Rao's method, we find a good technique to achieve matching, and we use this approach in our proposed method. Equation 1 shows the expression which is used in the matching.

$$S = \sum_{i,j \in I} \frac{1}{2} \left| sin\left(\alpha_{(i,j)} - \beta_{(i,j)}\right) \right| \quad (1)$$

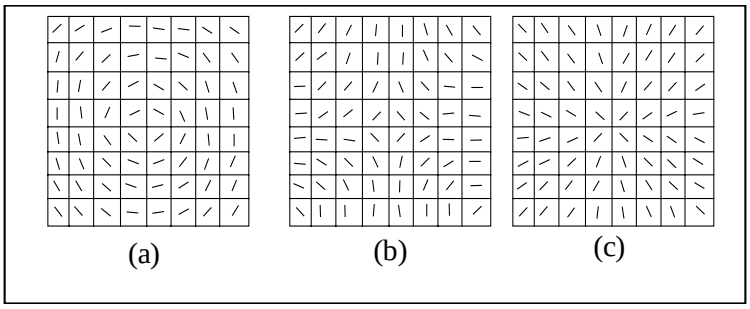

Figure 4. Three classes of templates to match flow-like patterns: (a) center; (b) saddle; and (c) node.

In equation 1, $\alpha_{(i,j)}$ and $\beta_{(i,j)}$ are the flow direction and template direction, respectively, at *(i,j)* position and *I* is the region of the template. According to Equation 1, *S* is smaller as the templates and patterns are equals. We note that in some matching, we can have a *S* minimal, but probably we do not have *S* = 0. Then, we should establish a certain threshold *Ts* to be the result of the matching *S*. In other words, all potential critical points whose values of matching *S* are less or equal to *Ts* should be considered a detected pattern in the original image.

To avoid noise and low resolution problems around the pattern's center, as we just discoursed, the matching is done only inside the limited area by the circles, as shown int the Figure 5.

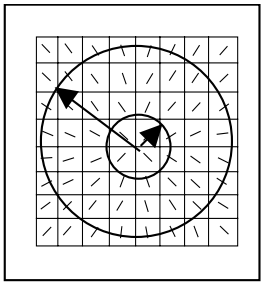

Figure 5. A template with two circled regions. The matching is done only inside the limited area by the two circles. This approach avoids bad resolution regions inside the small circle.

2.4 Dynamical systems estimating

In the final step, after we estimated the critical points positions and classes, we can estimate each found pattern with the Dynamical Systems which describe mathematically the pattern. Although, the templates used in the last step, had been sufficient to detect the position and the class of the desired pattern, many applications of oriented texture analysis like industrial inspection and even fluid flow, would wish a mathematical description of the these found patterns. This step would be called *symbolic description of the patterns*, as Rao's paper presents. In other words, when we have a texture oriented image we can find a synthetic image whose patterns are mathematical models of the original image.

$$\begin{bmatrix} \dot{x}_{i,j} \\ \dot{y}_{i,j} \end{bmatrix} = \begin{bmatrix} a_{11} & a_{12} \\ a_{21} & a_{22} \end{bmatrix} \begin{bmatrix} x_{i,j} \\ y_{i,j} \end{bmatrix} + \begin{bmatrix} t_{xi,j} \\ t_{y_{i,j}} \end{bmatrix} \tag{2}$$

$$\dot{v} = Av + t \tag{3}$$

To generate the synthetic image, we use the dynamical systems theory. Consider the differential equation system (2) and its general form (3), which may represent any pattern found in the last step. In this equation, the elements of $\dot{v} = [\dot{x}_{i,j}, \dot{y}_{i,j}]'$ are respectively the *Sx* and *Sy* responses of the Sobel operator at the first step of the proposed method, the elements of the vector $v = [x_{i,j}, y_{i,j}]'$ are the locations of the patterns in the original image and $t = [t_{x(i,j)}, t_{y(i,j)}]'$ allow some translation of the origin. The ***A*** matrix should be estimated according to the description of the found pattern, as exposed in Rao and Ford's papers. The ***A*** matrix may be estimated by minimizing:

$$\left(Av + t - \dot{v}\right)^2 = error^2 \tag{4}$$

The ***A*** matrix is estimated for each pattern found in the last step. Again, we calculate the values inside a circular region *W*, as showed in Fig. 5, but now, we vary the radius of the internal and external circles to obtain the best possible dimensions of the patterns.

3. RESULTS

In this section we present results of applying our methodology to several real images. These images have been selected from the domains of fluid flow visualization . The method was tested on a variety of experimental flow fields images, and four examples are included that illustrate the proposed methodology. The following parameters were fixed for all four experiments: the *W* circular region has inner radius *Ri* equal to *6* pixels length and outer radius *Ro* is equal *20* pixels length. So, the *W* circular region is inside a *40 x 40* area, in pixels. These values was chosen to be approximately the size of the expected patterns we wish to detect; we partition the *W* circular region about *36* areas, each one with a 10^o field of view for an operator of Fig. 2. All template sizes are *40 x 40* squared in pixels. Again this size was chosen according the size of patterns we wish to detect; the threshold *Ts = 60% of 1/S* when *S* is the result of a perfect matching between the pattern and template. Then, for a *40 x40* template, according Equation (1), *Ts* was fixed at *960*. The degree of monotonicity *Dm*, was chosen as 50%. In other words we labeled as potential critical points all points which have at least 50% of monotonicity around its center as just discoursed at Section 2.1. These parameters were selected throughout intuition and experimentation.

The first experiment is showed in Fig. 6. This is the same image was showed in Figure 1, where there are, in Figure 6.a, a cylindrical bar inside a flow fluid generating two vortexes , one saddle point and one occluded saddle point. Figure 6.b show in a sampled form the flow direction after step of the method, as just discoursed. Figure 6.c show the output of third step where we can see a set of candidates points which are circled. The concentration of false alarms is near real critical points. This is due the fixed degree of monotonicity we fixed

before. It occur in all the experiments. Figure 6.d show the final three patterns found, two vortex and one saddle point, as we circled. The occluded saddle point, which occur left beside of cylindrical bar was rejected as a pattern. As we just sad, we are not interested in this paper in partial occluded pattern, although we remark that our method may detect it too.

The second experiment, showed in Fig. 7, is a flow induced bay an oscillating cylinder. Where streamlines exist, this image has a strongly oriented texture that provides a low noise estimate of low orientation. There are about four vortexes near at each image's corner and about three partially occluded saddle point around the image's center. In Fig. 7.b we show, in a sampled form, the flow directions superimposed to the original image, Figure 7.a. In the Fig. 7.c we circled all candidates critical points found in the third step of the method. The output of the method, showed in the Fig. 7.d, is the four corner's vortex and one saddle point. This saddle point was detected because it is not totally occluded. We can detect the remainder of the partially occluded critical points as we change the experimental parameters. For example, if we change *Dm* from 50% to 45% or less or *Ts* from 60% or more, the remainder occluded critical points may be detected.

The third experiment is a simple flow noise image of only a node point. As we showed for all the experiments the Fig. 8.b show the flow directions in a sampled form. Fig. 8.b show the output of third step. This is a strongly oriented image with no occluded points and a unique patterns which is near the image bottom, so the *Ts* parameter of 960 and *Dm* of 50% is not ideal for this kind of image and we detect several of potential critical points, as showed Fig. 8.c by circled points. But, in the final step, as Fig. 8.d shows , the matching eliminated all these points and only the real critical point remainder.

In the fourth experiment we present a flow image with low coherence. This is a chaotic image and does not have well defined streamlines or a regular texture. In fact it is not clear to human observers which structures in the image are coherent, although there are clearly a vortex-like structure. Figure 9. We can see in the image only a center point and several occluded center and saddle points. In the Fig. 9.b we show the flow directions in a sampled form. Due low coherence for these fixed parameters we detect several potential critical points and in the output of the four step we see several critical points found. Some of these points are partial occluded points.

4. CONCLUSIONS

We proposed a method to detect and describe some kind of flow-like patterns. We use three principal steps in our method: flow direction detecting, potential critical points detecting and matching patterns. This approach have a relative low computational time. If the application require a mathematics description of the critical points found, we can include a four step in the and of the method estimating the differential equation system to each critical point achieved in the third step. The proposed methodology is based on current methods in the literature. In the future, we are interested in applying this method over turbulent flow blood outside of cardiac prothesis in a complete flow visualization system.

We can found floe-like patterns with fixed parameters which allow us to detect all kind of critical points if it's run at a coherent image with clear patterns structures. To these images we can work with a height *Dm* and *Ts* parameter. If the images have low coherence and not clear, to a human observers, pattern we should work with a relatively low *Dm* and *Ts* values, but we can not define all the flow-like structures detected.

The most computational time of the method is clearly the second step, potential critical points detecting. So, we suggest to parallelise these step to accelerate the method. We plan to pursue this direction of research in the future.

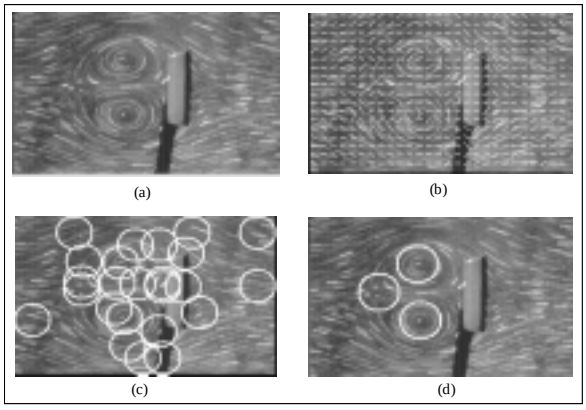

Figure 6. A cylindrical bar inside a flow fluid generating patterns. (a) original image; (b) flow directions showed in a sampled form to avoid clutter; (c) potential critical points detected; (d) final patterns found: two center and one saddle point.

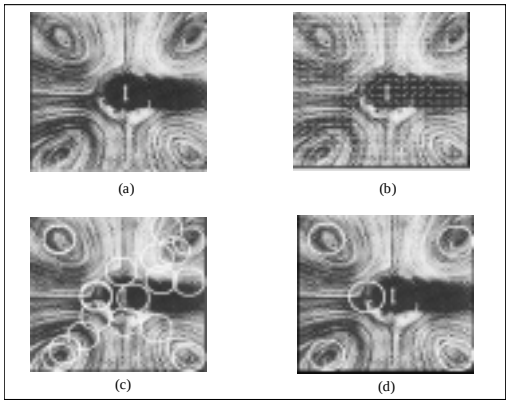

Figure 7. A flow induced by an oscillating cylinder. (a) original image; (b) flow directions showed in a sampled form to avoid clutter; (c) potential critical points detected; (d) final patterns found: four flow-like vortexes and one partially occluded saddle point near the image's center.

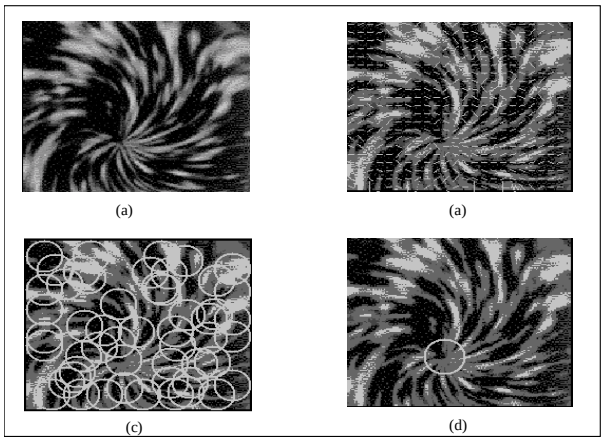

Figure 8. A height coherent image of a node point. (a) original image; (b) flow directions showed in a sampled form to avoid clutter; (c) potential critical points detected. Due *Ts* and *Dm* parameters the algorithm detected many false potential patterns; (d) final patterns found: one node point.

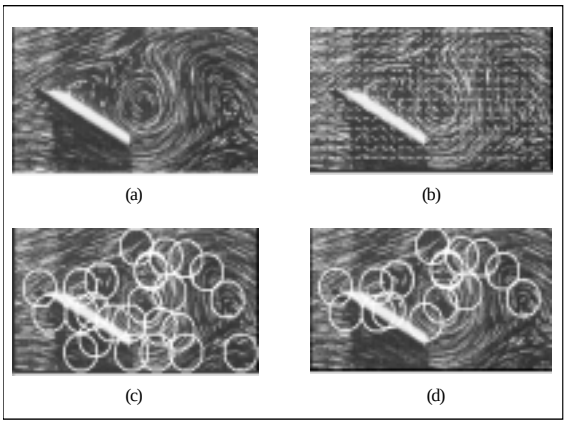

Figure 9. A low coherence image with many not clear patterns. (a) original image; (b) flow directions showed in a sampled form to avoid clutter; (c) potential critical points detected; (d) the algorithm detected a center patterns and many others occluded patterns and not clear structures.

Acknowledgments

The authors are grateful to CNPq, CAPES and FAPEMIG for the financial support to this project.

REFERENCES

D. K. Arrowsmith and C. M. Place, 1992. *Dynamical Systems: Diferential Equations, Maps and Chaotic Behavior*, Chapman and Hall, New York.

R. Conners, C. W. McMillin, K. Lin and R. E. Vasquez-Espinosa, 1983. *Identifying and locating surface defects in wood: Part of an automated lumber processing system*, IEEE Trans. on PAMI 5, pp. 573-582.

H. Core, W. Cote and A. Day, 1979. *Wood Structure and Identification*, Syracure University Press, Syracure.

W. Erteld, H. Mette and W. Achterberg, 1964. *Defects in Wood*, Leonard Hill, London.

R. M. Ford, 1997. *Critical Point Detection in Fluid Flow Images Using Dinamical Systems Properties*, Pattern Recognition. 30, no. 12, pp. 1991-2000.

Fractography features revealed by light microscopy, in Metals Handbook, vol. 9: Fractography and Atlas of Fractographys (8th ed.). Metals Park, OH: Amer. Soc. Metals.

W. T. Freeman and E. H. Adelson, 1991. *The design and use of steerable filters*, IEEE Trans. on PAMI 13(9), pp. 891-906.

V. F. Kopiev, M. Yu. Zaitsev, L. P. Guriashkin, and V. A. Yakovlev, 1996. *A Thecnique for Visualization of the Turbulent Vortex Ring*. Atlas of Visualization II, Chapter eight, The Visualization Society of Japan.

W. S. MackKenzie, 1982. *Atlas of Ingeneous Rocks and Their Textures*, Wiley, New York.

Z. Mao, 1992. *Computing optical flow in rigid and nonrigid object motion*, Ph.D. Thesis, Department of Electrical and Computer Engineering, University of Arizona, Arizona.

L. A. S. B. Martins and J. H. Whitelaw, 1996. *Visualization of the Flow Into and Out of Hole in a Duct Wall*, Atlas of Visualization II, Chapter two, The Visualization Society of Japan.

A. Panshin, C. D. Zeeuw and H. Brown, 1964. *Textbook of Wood Technology*, McGraw Hill, New York.

X. Qinghan and B. Zhaoqi, 1986. *An appoach to fingerprint by using the atributes of feature lines of fingerprints*, in Eight Int. Conf. Patt. Recognition, Oct., pp. 663-665.

Rao, A. R. and Jain, R. C., 1992. *Computerized Flow Filed Analysis: Oriented Texture Fields*, IEEE Transactions on Patterns Analysis and Machine Inteligence, vol. 14, no. 7, july.

A. R. Rao and R. Jain, 1990. *A classification scheme for visual defects arising in semiconductor wafer inspection*, J. Crystal Growth, vol. 103, pp. 398-406.

A. R. Rao and B. G. Schunk, 1991. *Computing oriented textures fields*, CVGIP: Graphical Models Image Process. 53(2), 157-185.

S. Smale and M. W. Hirsch, 1974. *Differential Equations, Dynamical Systems and Linear Algebra*, Academic Press, New York.